J.Natn.Sci.Foundation Sri Lanka 2025 53 (4): 437 - 445
DOI: http://dx.doi.org/10.4038/jnsfsr.v53i4.12659

RESEARCH ARTICLE

Biomedical Instrumentation

Chest anteroposterior diameter measurement: Comparison of ultrasonic and manual methods across different BMI categories

C Muralidharan * and MC Jobin Christ
Department of Biomedical Engineering, Rajalakshmi Engineering College, Anna University, Chennai, India.

Submitted: 29 April 2025; Revised: 22 September 2025; Accepted: 14 November 2025

Abstract: Chest anteroposterior diameter (APD) measurement is a critical metric in evaluating thoracic dimensions, particularly in assessing conditions like pectus excavatum and guiding interventions such as laryngoscopy and cardiopulmonary resuscitation. The lateral distance measurement of the thoracic cavity using the computed tomography image provides APD, but they expose the subject to radiation. Though the manual method of chest APD measurement using a wooden ruler is radiation-free, it is time-consuming and prone to human errors. This study proposes a novel and radiation-free method of measuring chest APD using an ultrasonic sensor. The accuracy and reliability of the measured chest APD using the ultrasonic method were compared with the manual method across three distinct BMI categories of 150 participants. The measured chest APD using ultrasonic and manual methods for underweight, normal, and obese participants ranges from 17-18 cm, 18.5-20.5 cm, and 23.75-25 cm, respectively. The statistical analyses, including paired t-tests and intra-class correlation coefficients (ICC), were performed to assess agreement between the two methods. The paired t-test manifests no significant difference between the mean APD measured using ultrasonic and manual methods with p-values of 0.8742 (underweight), 0.7390 (normal), and 0.7998 (obese). The ICC values obtained from the intra- and inter-observers for the ultrasonic and manual methods were ICC ≥ 0.93, $0.80 \leq \text{ICC} \leq 0.82$ and 0.91, and 0.78. The ICC value obtained from the intra- and inter-observers for the ultrasonic method was high, so the ultrasonic method is better than the manual method. This study concludes that the ultrasonic method provides a radiation-free alternative to the manual method, making it suitable for routine clinical use globally.

Keywords: Arduino Uno, body mass index, chest anteroposterior diameter, paired t-test, ultrasonic sensor.

INTRODUCTION

The chest anteroposterior diameter (APD) is the distance between the midpoint on the lower half of the sternum's anterior skin and the posterior skin on the spinal process of the spine (Pickard et al., 2006; Meyer et al., 2010; Lee et al., 2019; Kim et al., 2020). The chest APD is used to assess the severity of pectus excavatum, a chest wall deformity (Haller et al., 1987; Lain et al., 2017; Biovati et al., 2020; Tro et al., 2022). An observational study suggested that during laryngoscopy the pillow height be adjusted manually, according to the chest APD (El-Orbany et al., 2011; Choi et al., 2013; Apfelbaum et al., 2021). A finite element simulation study showed that during cardiopulmonary resuscitation (CPR), to achieve a fixed compression depth, the compression force must be increased or decreased according to the chest APD (Moradicheghamahi et al., 2023). According to the guidelines of the American Heart Association for performing effective cardiopulmonary resuscitation (CPR), the compression depth achieved for adults, children, and infants is equal to one-third of their chest APD (Kao et al., 2009; Marino et al., 2018; Panchal et al., 2020). Several studies also suggested that the chest APD varies due to age, body mass index, and disease conditions. (Lee et al., 2015; Yoo et al., 2018; Sarkar et al., 2019; Chavan et al., 2021; Atiksawedparit et al., 2023). computed tomography (CT) of the chest offers a precise way to measure the chest APD and evaluate the chest wall structure. This involves drawing a line from the anterior

* Corresponding author (muralidharan.c@rajalakshmi.edu.in; https://orcid.org/0009-0009-4609-1597)

side of the lower half of the sternum to the posterior side of the spine on the CT image. The length of the line provides the APD (Zarb et al., 2010; Jin et al., 2016). The amount of radiation dose delivered to the patient during CT ranges from 4 to 7 millisieverts (ICRP, 2007; McCollough et al., 2008). However, taking multiple CT scans exposes the patients to harmful ionising radiation that changes the structures of DNA and chromosomes, which leads to a risk of cancer (Zhou et al., 2019; Devic et al., 2022). The calliper-based external measurement technique is also used to measure the chest APD (Ewert et al., 2017; Chen et al., 2022). This method is more affordable than a CT scan, but reproducibility between different persons in measurement is not established. The manual method of measuring chest APD is by using a wooden ruler. In this method the participant is allowed to rest in a supine position on a flat surface. The wooden ruler is placed perpendicular to the nipple line and spine. The distance between the nipple and spine is measured as chest APD. It is important to note that this manual method is time-consuming and also results in human error in measurement. The proposed study is a reliable, error-free alternative method of measuring the chest APD using an ultrasonic sensor. The sound waves generated from the ultrasonic sensor are non-ionising in nature. They are not harmful to humans like the electromagnetic waves from X-rays and CT. The aim is to verify the accuracy and robustness of the proposed ultrasonic method by validating its findings with those obtained through the manual method. This comparison is conducted across three distinct groups, categorised as underweight, normal, and obese, based on participants' BMI values.

MATERIALS AND METHODS

A prototype of a mechanical setup for mounting the ultrasonic sensor was designed and modelled using SolidWorks for this study. Figures 1, 2, and 3 are the front, side, and top views, of CAD design models of the mechanical setup. The mechanical setup was fabricated using mild steel material (Yan et al., 2014). All the dimensions mentioned in the three views were in inches.

The isometric view of the mechanical setup in Figure 4 consists of a metallic frame. The metallic frame was supported through rods.

The anteroposterior diameter of the human participant is measured through the HC-SR04 ultrasonic distance

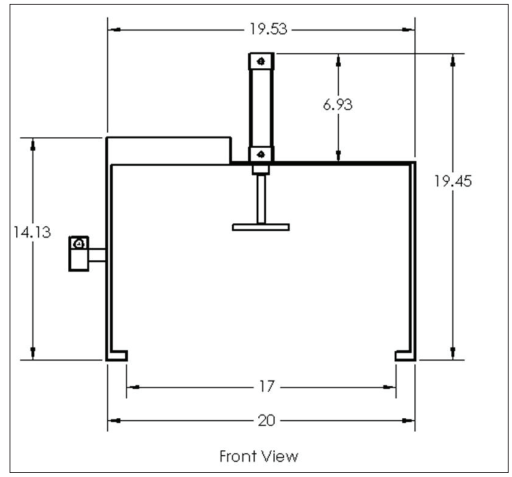

Figure 1: Front view of the mechanical setup

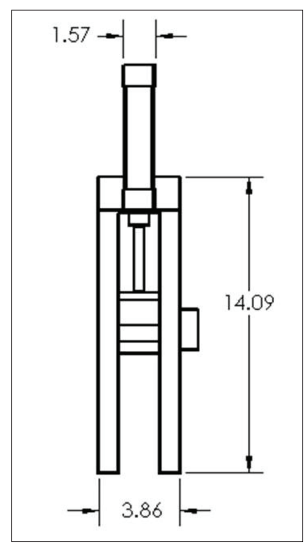

Figure 2: Side view of the mechanical setup

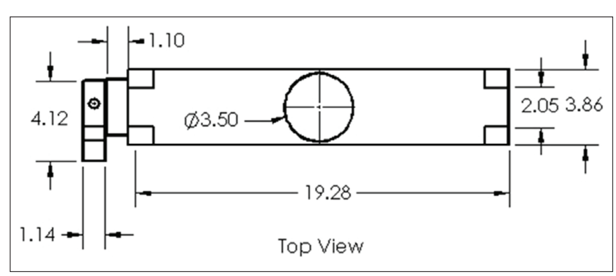

Figure 3: Top view of the mechanical setup

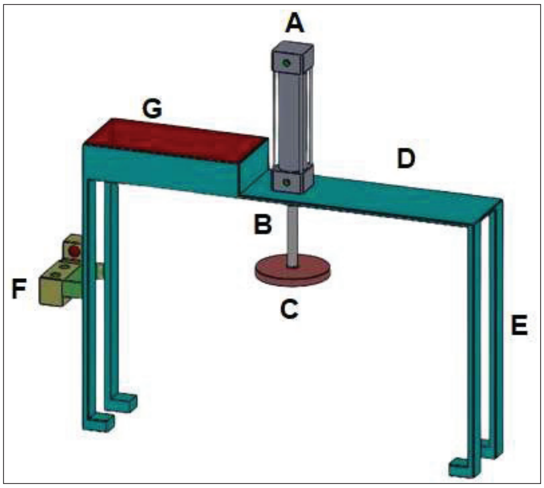

Figure 4: Isometric view of the mechanical setup (A- Pneumatic cylinder, B- Piston rod, C- Compression pad, D- Metallic frame, E- Rods, F- Solenoid valve, G- Electronic hardware setup)

sensor. Figure 5 shows the HC-SR04 ultrasonic distance sensor (Lumbanbatu et al., 2024). This is a widely used ultrasonic distance sensor capable of measuring non-contact distances ranging from 2 to 400 cm, with an accuracy of up to 3 mm. It operates using sonar technology to calculate the distance to an object. The HC-SR04 is compact, simple to set up, and features four pins for power, trigger, echo, and ground. Additionally, it includes control circuitry to ensure reliable and consistent data.

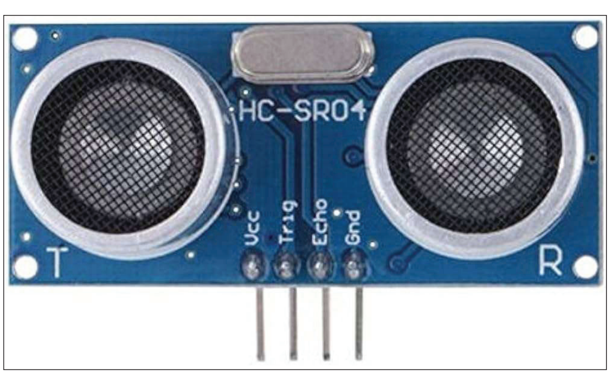

Figure 5: HC-SR04 ultrasonic sensor

The Arduino Uno microcontroller board in Figure 6 is used to interface the HC-SR04 ultrasonic distance sensor. This board features both digital and analogue input/output (I/O) pins, allowing it to connect with various expansion boards and other circuits. It includes 14 digital I/O pins and 6 analogue I/O pins. The board can be programmed using the Arduino IDE (integrated development environment) via a type B USB cable and can be powered either through a USB connection or a barrel connector that accepts voltages between 7 and 20 volts, such as a 9 volt battery.

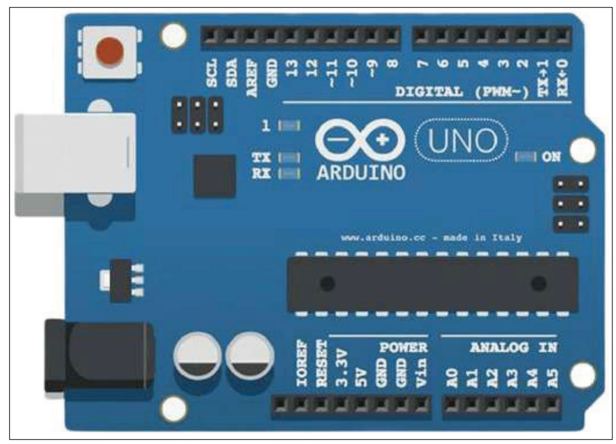

Figure 6: Arduino Uno Board

Participant selection criteria

The 200 participants of varying age groups—young (20–35), middle (35–55), and old (56 or above), participated in the study. Out of 200 participants, 150 males were selected for the study, based on the inclusion criteria. The inclusion criteria are healthy individuals with BMI < 18.5 kg/m², 18.5 kg/m² < BMI < 25 kg/m², and 25 kg/m² < BMI < 30 kg/m². The remaining 50 participants were not selected for the study, based on the exclusion criteria. The exclusion criteria are unhealthy individuals having cardiac illness, chest injury, or spinal scoliosis, and females, including pregnant women. The selected 150 participants were grouped into underweight (BMI < 18.5 kg/m²), normal (18.5 kg/m² < BMI < 25 kg/m²), and obese (25 kg/m² < BMI < 30 kg/m²) based on the World Health Organization (WHO) guidelines (Lad et al., 2012). There were 50 participants in the underweight group, with a mean age of 26.32 ± 5.78, a mean height of 152.77 cm ± 2.06 cm, and a mean weight of 41.52 kg ± 1.27 kg. Similarly, in the normal group, there were 50 participants with a mean age of 25.2 ± 6.50, a mean height of 172.86 cm ± 6.88 cm, and a mean weight of 67.50 kg ± 6.68 kg. Meanwhile, there were 50 participants in the obese group, with a mean age of 28.9 ± 9.28, a mean height of 167.24 cm ± 5.73 cm, and a mean weight of 86.53 kg ± 6.60 kg.

Ethical clearance

The study involving human participants was reviewed and approved by the Rajalakshmi Engineering College ethical committee (REC/IEC/005/2024). The participants also gave written informed consent to take part in this study.

Measurement protocol

The observer A and observer B performed chest anterior-posterior diameter (APD) measurements using two methods: the ultrasonic and the manual method. Observer A was the anthropometrist, and observer B was the researcher (author 1). The measurements were carried out based on the guidelines provided by the ethical committee members. In the inter-observer protocol, both observers measured chest APD on each participant only once (for each method) in the same session, under identical conditions. In the intra-observer protocol, each observer repeated the chest APD measurements on all participants one week later. The same protocol and equipment were used; observers were blind to their first measurements when re-measuring.

Ultrasonic sensor method

Figure 7 demonstrates the method of measuring the chest anteroposterior diameter of human participants using an HC-SR04 ultrasonic sensor. When the microcontroller in the Arduino Uno board sends a signal on pin number 5 to the HC-SR04 ultrasonic sensor, it triggers the ultrasonic sensor. The triggering action causes the transmitter module of the HC-SR04 to generate an ultrasonic wave. This wave travels to the participant's anterior chest, reflects off the surface, and returns back to the HC-SR04 sensor's receiver module, changing the echo pin from low to high. The time taken (t) for the ultrasonic wave to travel to the chest and reflect back is the time duration of the echo pin to change from low to high. The time duration (t) is determined using the precision timer available in the microcontroller of an Arduino Uno board. The distance (B) between the sensor and the anterior side of the chest is then computed using the time duration (t) and velocity of the ultrasonic wave (v) using equation 1.

$$B = v \times t \qquad ...(1)$$

where
v = Velocity of ultrasonic waves in air (0.034 cm/µs)
t = Time taken to transmit and receive the ultrasonic waves (µs)

The distance from the ultrasonic sensor to the posterior side of the thoracic cavity of the human participant is fixed as A. The anteroposterior diameter (APD) is then computed using the A and B values from equation 2.

$$APD = A - B \qquad ...(2)$$

Where APD, A and B are measured in centimetres (cm)

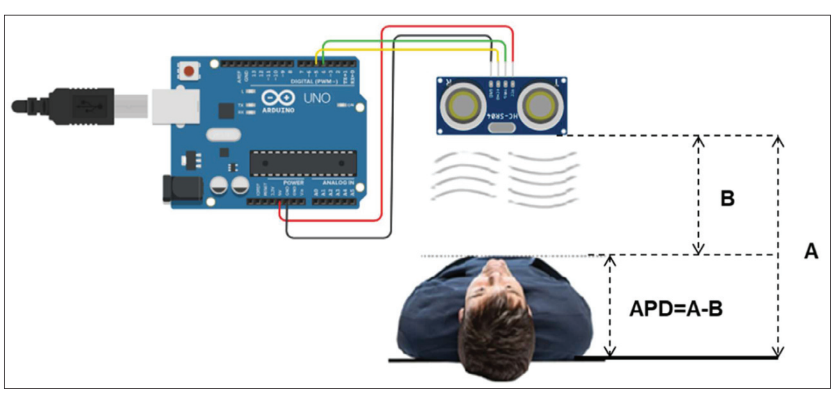

Figure 7: Anteroposterior diameter (APD) measurement using the ultrasonic method (A - the distance from the ultrasonic sensor to the posterior side of the thoracic cavity of the human, B - the distance between the sensor and the anterior side of the chest)

Figure 8 shows the placement of the ultrasonic sensor in the mechanical setup for chest APD measurement. The participant is allowed to lie in a supine position on the table. The mechanical setup was fixed on the table such that the patient's safety is ensured. The HC-SR04 ultrasonic sensor was affixed to the bottom side of its frame, ensuring it was directed towards the central region between the xiphoid and manubrium of the participant. The chest APD value of the individual participant measured using the ultrasonic method is by measuring the A and B value. The B value is measured through 10 trials for each participant and calculated their corresponding average and available as average B in cm. The A value is fixed as 28 cm. The APD is then measured using the formula APD = A-B. The same procedure is repeated to measure the APD values for 50 participants in each group to a total of 150 participants in 3 groups. Technical expertise is required to position the ultrasonic sensor to the lower half of the participant's sternum for measuring the chest APD.

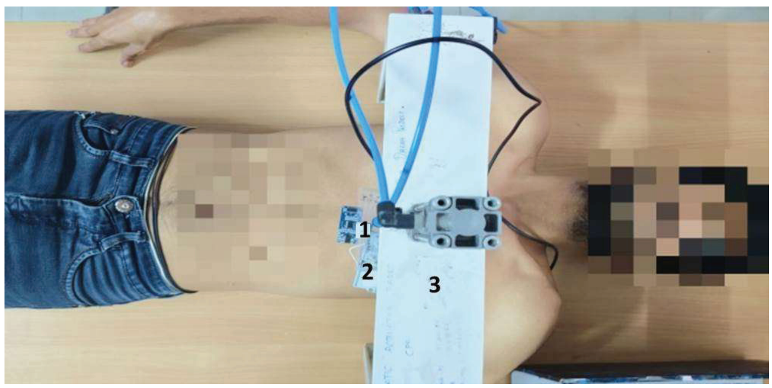

Figure 8: Ultrasonic sensor placements for anteroposterior diameter (APD) measurement- 1. Ultrasonic sensor 2. Arduino Uno board 3. Metallic frame

Validation

The measured APD values of all the 150 participants available in three groups were validated using the manual method. In this method a piece of cardboard is placed over the participant's chest. The lateral distance from the posterior side of the spine to the midpoint between the xiphoid and manubrium of the sternum is measured using a wooden ruler as shown in Figure 9. This method provides a direct means of quantifying the chest anteroposterior diameter (APD). The accuracy of the manual method is improved by using a calibrated digital ruler instead of an analogue wooden ruler.

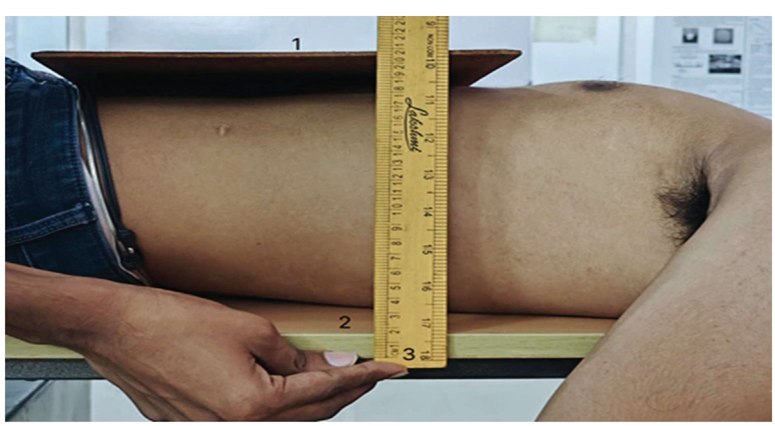

Figure 9: APD measurement using the manual method

Statistical tests and plots

The Statistical Package for Social Sciences (SPSS) statistical tool was used for testing the measured chest APD using the ultrasonic method and the manual method. The paired t-test was used to compare the mean APD measured using the ultrasonic and manual methods. The null hypothesis (H_0): no significant difference between the mean values of the APD measured by ultrasonic and manual methods. The alternative hypothesis (H_1): significant difference between the mean values of APD measurement between the two measurement methods. The significance level was set at $p > 0.05$. The scatter plot was plotted to visualise the correlation and overall relationship between the two methods for underweight, normal, and obese group participants. The intra-class correlation coefficient was also computed to assess the consistency or agreement of APD measurements made by both the inter-observer and the intra-observer.

RESULTS AND DISCUSSION

The measured chest APD using ultrasonic and manual methods for underweight, normal, and obese group participants were in the ranges 17 - 18 cm, 18.5 - 20.5 cm, and 23.75 - 25 cm, respectively. The scatter plots were plotted for underweight, normal and obese group participants, using the chest APD measured from ultrasonic and manual methods, in Figures 10(a), 10(b), and 10(c), respectively. A few data points in the scatter plot of the underweight group participants fall along the trend line, and others fall away from the trend line. But for normal and obese group participants, most of the data points fall along the trend line. The correlation coefficients for the scatter plots plotted for underweight, normal, and obese participants in Figures 10(a), 10(b), and 10(c) were 0.6234, 0.9788, and 0.8057 respectively.

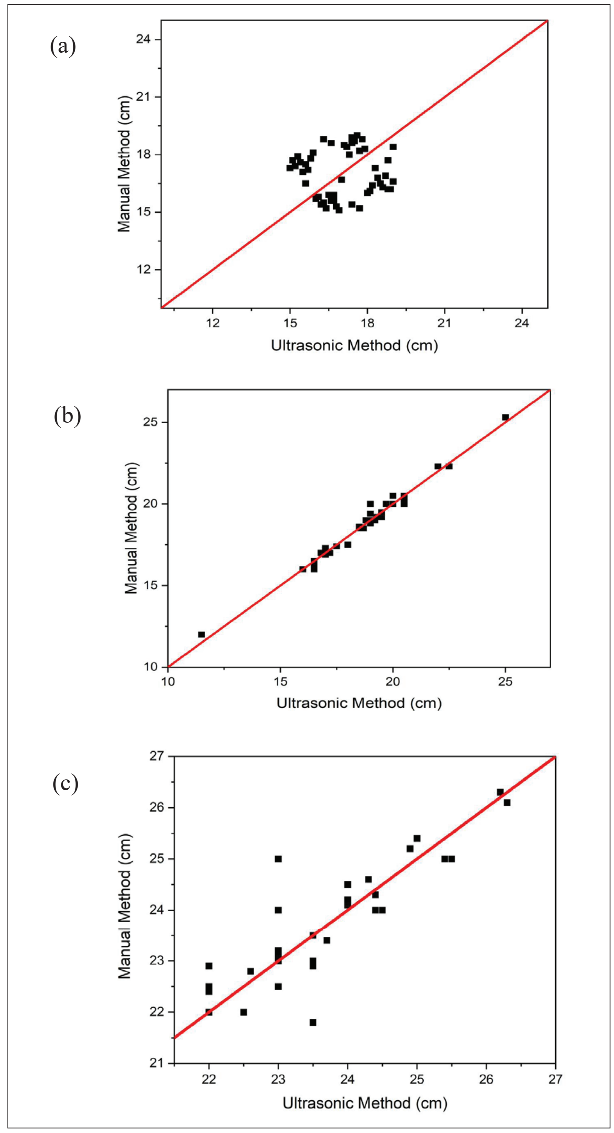

Figure 10: Comparison between chest APD measurements of Ultrasonic and Manual methods a. Underweight participant's b. Normal participant's c. Obese participant's

Table 1: Paired t-test results for underweight, normal and obese groups

Parameters and Values	MM-UWG	UM-UWG	MM-NG	UM-NG	MM-OG	UM-OG
Age	26.32 ± 5.78	26.32 ± 5.78	25.2 ± 6.5	25.2 ± 6.5	28.9 ± 9.3	28.9 ± 9.3
Height (cm)	152.77 ± 2.06	152.77 ± 2.06	172.86 ± 6.88	172.86 ± 6.88	167.24 ± 5.73	167.24 ± 5.73
Weight (kg)	41.52 ± 1.27	41.52 ± 1.27	67.5 ± 6.7	67.5 ± 6.7	86.53 ± 6.60	86.53 ± 6.60
APD (cm)	17.05 ± 1.17	17.01 ± 1.21	18.57 ± 2.03	18.55 ± 2.02	23.75 ± 1.22	23.73 ± 1.24
P-value	0.8742		0.7391		0.7998	
t-statistic	0.1590		0.3349		0.2549	

According to Table 1, the mean APD values obtained from the paired t-test for the underweight, normal, and obese group participants using the manual and ultrasonic sensor methods were 17.05 ± 1.17 cm and 17.01 ± 1.21 cm, 18.57 ± 2.03 cm and 18.55 ± 2.02 cm, 23.75 ± 1.22 cm, and 23.73 ± 1.24 cm, respectively. In the underweight group, the paired t-test results yielded a t-statistic value and high p-value (t-statistic = 0.1590 and $p = 0.8743$, $p > 0.05$). Meanwhile, in the normal group, the test results yielded a t-statistic value that is much less than the p value (t-statistic = 0.3349 and $p = 0.7391$, $p > 0.05$). Similarly, for the obese group, the test results also yielded a t-statistic value that is less than the p-value (t-statistic =0.2549 and $p = 0.7998$, $p > 0.05$). The intra-observer ICC values obtained from observers A and B for the ultrasonic method were 0.93 and 0.95. Similarly, the intra-observer ICC values obtained from observers A and B for the manual method were 0.80 and 0.82. Meanwhile, the inter-observer ICC values obtained from observers A and B for the ultrasonic and manual methods were 0.91 and 0.78, respectively. The measured chest APD using both the methods was normally distributed.

The paired t-test results in Table 2 indicated that there is no significant difference ($p > 0.05$) in APD measurements between the two measurement methods for the underweight, normal, and obese groups. The high P-value ($p > 0.05$) reinforces the null hypothesis, which posits no significant difference between the APD measured using ultrasonic and manual methods. The correlation coefficients obtained from the scatter plots of the underweight, normal, and obese group show a good correlation between the two methods. Similarly, it is especially evident that the majority of data points align along the trend lines for the underweight, normal, and obese groups. This alignment with the trend lines indicates that the measurements from the two methods are very similar, with minimal systematic bias. The ultrasonic method showed excellent intra-observer reliability for observer A (anthropometrist) and observer B (researcher) (ICCs ≥ 0.93), while the manual method showed only adequate reliability ($0.80 \leq \text{ICC} \leq 0.82$), with higher variability. The inter-observer agreement was similarly better in the ultrasonic method (ICC=0.91) compared to the manual method (ICC=0.78). Thus, for precise chest APD measurements, particularly in populations with different body types (underweight, normal, and obese), the ultrasonic method is preferred. The manual method can be used for the screening process.

CONCLUSION

The experimental study concludes that the ultrasonic sensor method measures the chest anteroposterior diameter for underweight, normal, and obese participants effectively. The ultrasonic waves generated from the ultrasonic sensor produce non-ionising radiation. Meanwhile, measuring the chest APD using the manual method results in human error. Similarly, the X-rays generated in the CT methods produce ionising radiation. Measuring the chest APD provides insight into the anatomy of the thorax and respiratory health. The changes in APD due to chronic obstructive pulmonary diseases like asthma, pulmonary fibrosis, and emphysema can be easily detected. Congenital chest wall deformation, like pectus excavatum or pectus carinatum, can also be detected using the chest APD. The early measurement of chest APD avoids the surgical procedure to overcome the severe deformation of the chest wall.

The limitations of our study are that, whenever the human participant is not positioned in the line of sight of the ultrasonic sensor, the ultrasonic signal deflected away rather than reflected back to the ultrasonic sensor. In this scenario, the calculated chest APD is incorrect. While measuring the chest APD, the participant should not wear any fabrics, because fabrics absorb the ultrasonic signal. The room used for measuring chest APD should be free from air conditioners and ceiling fans, because the ultrasonic sensor absorbs the acoustic signals and pulse signals generated by air conditioners and ceiling fans.

Future work

The future work of our research will be deputising a female observer and supervisor for measuring the chest APD of female participants using the same setup and protocol. This concept of measuring the chest APD will be incorporated in a simple chest compression device. And then, based on the measured the chest APD modelling and designing will be done to produce different types of CPR manikins. These CPR manikins will mimic the underweight, normal and obese participants. This simple chest compression device will be programmed to perform CPR on the manikins to achieve a compression depth of $1/3^{rd}$ of chest APD of the manikins resulting in effective CPR. This simple mechanical chest compression device will replace the existing mechanical CPR devices and perform effective CPR across different BMI categories.

REFERENCES

Apfelbaum, J. L., Hagberg, C. A., Connis, R. T., Abdelmalak, B. B., Agarkar, M., Dutton, R. P., *et al.* (2021). 2022 American Society of Anesthesiologists practice guidelines for management of the difficult airway. *Anesthesiology*, *136*(1), 31-81. https://doi.org/10.1097/aln.0000000000004002

Atiksawedparit, P., Sathapornthanasin, T., Chalermdamrichai, P., Sanguanwit, P., Saksobhavivat, N., Saelee, R., & Phattharapornjaroen, P. (2023). Using computed tomography to evaluate proper chest compression depth for cardiopulmonary resuscitation in Thai population: A retrospective cross-sectional study. *Plos One*, *18*(2), e0279056. https://doi.org/10.1371/journal.pone.0279056

Biavati, M., Kozlitina, J., Alder, A. C., Foglia, R., McColl, R. W., Peshock, R. M., Kelly Jr, R. E., Kim Garcia, C. (2020). Prevalence of pectus excavatum in an adult population-based cohort estimated from radiographic indices of chest wall shape. *Plos One*, *15*(5), e0232575. https://doi.org/10.1371/journal.pone.0232575

Chavan, S. D., Patil, V. S., & Patil, B. K. (2021). Comparison of thoracic dimensions of chronic obstructive pulmonary disease patients and healthy controls: A cross-sectional study. *International Journal of Advanced Research in Medicine*, *3*, 75-77. https://doi.org/10.22271/27069567.2021.v3.i1b.105

Chen, T., Chen, C., Zeng, Q., Zhang, Y., Jiao, J., Zhang, X., *et al.* (2022). Use of caliper-based external measurement of body surface in assessing the severity of pectus excavatum. *Frontiers in Pediatrics*, *10*, 1015026. https://doi.org/10.3389/fped.2022.1015026

Choi, J. W., Kim, J. A., Kim, H. K., Oh, M. S., & Kim, D. K. (2013). Chest anteroposterior diameter affects difficulty of laryngoscopy for non-morbidly obese patients. *Journal of Anesthesia*, *27*, 563-568. https://doi.org/10.1007/s00540-013-1572-1

Devic, C., Bodgi, L., Sonzogni, L., Pilleul, F., Ribot, H., Charry, C., Le Moigne, F., Paul, D., Carbillet, F., Munier, M., & Foray, N. (2022). Influence of cellular models and individual factor in the biological response to chest CT scan exams. *European radiology experimental*, *6*(1), 14. https://doi.org/10.1186/s41747-022-00266-0

El-Orbany, M., Woehlck, H., & Salem, M. R. (2011). Head and neck position for direct laryngoscopy. *Anesthesia & Analgesia*, *113*(1), 103-109. https://doi.org/10.1213/ANE.0b013e31821c7e9c

Ewert, F., Syed, J., Wagner, S., Besendoerfer, M., Carbon, R. T., & Schulz-Drost, S. (2017). Does an external chest wall measurement correlate with a CT-based measurement in patients with chest wall deformities. *Journal of Pediatric Surgery*, *52*(10), 1583-1590. https://doi.org/10.1016/j.jpedsurg.2017.04.011

Haller, J. A., Kramer, S. S., & Lietman, S. A. (1987). Use of CT scans in selection of patients for pectus excavatum surgery: a preliminary report. *Journal of Pediatric Surgery*, *22*(10), 904-906. https://doi.org/10.1016/s0022-3468(87)80585-7

Jin, S. Y., Oh, S. B., & Kim, Y. O. (2016). Estimation of optimal pediatric chest compression depth by using computed tomography. *Clinical and Experimental Emergency Medicine*, *3*(1), 27. https://doi.org/10.15441/ceem.16.119

Kao, P. C., Chiang, W. C., Yang, C. W., Chen, S. J., Liu, Y. P., Lee, C. C., *et al.* (2009). What is the correct depth of chest compression for infants and children? A radiological study. *Pediatrics*, *124*(1), 49-55. https://doi.org/10.1542/peds.2008-2536

Kim, Y. H., Lee, J. H., Lee, D. W., Song, Y. G., Lee, K. Y., Lee, Y. H., *et al.* (2020). Applicability of anatomical landmarks for chest compression depth in cardiopulmonary resuscitation for children. *Scientific Reports*, *10*(1), 1921. https://doi.org/10.1038/s41598-020-58649-5

Lad, U. P., Satyanarayana, P., Shisode-Lad, S., Siri, C. C., & Kumari, N. R. (2012). A study on the correlation between the body mass index (BMI), the body fat percentage, the handgrip strength and the handgrip endurance in underweight, normal weight and overweight adolescents. *Journal of Clinical and Diagnostic Research: JCDR*, *7*(1), 51. https://doi.org/10.7860/JCDR/2012/5026.2668

Lain, A., Garcia, L., Gine, C., Tiffet, O., & Lopez, M. (2017). New methods for imaging evaluation of chest wall deformities. *Frontiers in Pediatrics*, *5*, 257. https://doi.org/10.3389/fped.2017.00257

Lee, H., Oh, J., Lee, J., Kang, H., Lim, T. H., Ko, B. S., *et al.* (2019). Retrospective study using computed tomography to compare sufficient chest compression depth for cardiopulmonary resuscitation in obese patients. *Journal of the American Heart Association*, *8*(23), e013948. https://doi.org/10.1161/jaha.119.013948

Lee, S. H., Kim, D. H., Kang, T. S., Kang, C., Jeong, J. H., Kim, S. C., & Kim, D. S. (2015). The uniform chest compression depth of 50 mm or greater recommended by current guidelines is not appropriate for all adults. *The American Journal of Emergency Medicine*, *33*(8), 1037-1041. https://doi.org/10.1016/j.ajem.2015.04.034

Lumbanbatu, E. M., Hamdani, D., & Setiawan, I. (2024). Development of Arduino Uno-Based Doppler Effect Trainer with FC-04 Sensor and HCSR-04 Sensor in Senior High School. *Asian Journal of Science Education*, *6*(1), 34-45. https://doi.org/10.24815/ajse.v6i1.35884

Marino, B. S., Tabbutt, S., MacLaren, G., Hazinski, M. F., Adatia, I., Atkins, D. L., *et al.* (2018). Cardiopulmonary resuscitation in infants and children with cardiac disease: a scientific statement from the American Heart Association. *Circulation*, *137*(22), e691-e782. https://doi.org/10.1161/CIR.0000000000000524

McCollough, C., Cody, D., Edyvean, S., Geise, R., Gould, B., Keat, N., Huda, W., Judy, P., Kalender, W., McNitt-Gray, M., *et al.* (2008). The Measurement, Reporting, and Management of Radiation Dose in CT; Report of AAPM Task Group; *American Association of Physicists in Medicine*: Alexandria, VA, USA; Volume 23, pp. 1–28. https://doi.org/10.37206/97

Meyer, A., Nadkarni, V., Pollock, A., Babbs, C., Nishisaki, A., Braga, M., *et al.* (2010). Evaluation of the Neonatal Resuscitation Program's recommended chest compression depth using computerized tomography imaging. *Resuscitation*, *81*(5), 544-548. https://doi.org/10.1016/j.resuscitation.2010.01.032

Moradicheghamahi, J., Fortuny, G., López, J. M., Puigjaner, D., Herrero, J., & Azeli, Y. (2023). The effect of thoracic dimensions on compression depth during cardiopulmonary resuscitation. *International Journal for Numerical Methods in Biomedical Engineering*, *39*(7), e3718. https://doi.org/10.1002/cnm.3718

Panchal, A. R., Bartos, J. A., Cabañas, J. G., Donnino, M. W., Drennan, I. R., Hirsch, K. G., *et al.* (2020). Part 3: adult basic and advanced life support: 2020 American Heart Association guidelines for cardiopulmonary resuscitation and emergency cardiovascular care. *Circulation*, *142*(16_Suppl_2), S366-S468. DOI: https://doi.org/10.1161/cir.0000000000000901

Pickard, A., Darby, M., & Soar, J. (2006). Radiological assessment of the adult chest: implications for chest compressions. *Resuscitation*, *71*(3), 387-390. https://doi.org/10.1016/j.resuscitation.2006.04.012

Sarkar, M., Bhardwaz, R., Madabhavi, I., & Modi, M. (2019). Physical signs in patients with chronic obstructive pulmonary disease. *Lung India*, *36*(1), 38-47. https://doi.org/10.4103/lungindia.lungindia_145_18

The 2007 Recommendations of the International Commission on Radiological Protection. *ICRP publication* 103. Ann. ICRP 2007, *37*, 1–332. https://doi.org/10.1016/j.icrp.2007.10.003

Trò, R., Martini, S., Stagnaro, N., Sambuceti, V., Torre, M., & Fato, M. M. (2022). A new tool for assessing Pectus Excavatum by a semi-automatic image processing pipeline calculating the classical severity indexes and a new marker: the Volumetric Correction Index. *BMC Medical Imaging*, *22*(1), 30. https://doi.org/10.1186/s12880-022-00754-0

Yan, J. B., Liew, J. R., Zhang, M. H., & Wang, J. Y. (2014). Mechanical properties of normal strength mild steel and high strength steel S690 in low temperature relevant to Arctic environment. *Materials & Design*, *61*, 150-159. https://doi.org/10.1016/j.matdes.2014.04.057

Yoo, K. H., Oh, J., Lee, H., Lee, J., Kang, H., Lim, T. H., et al. (2018). Comparison of heart proportions compressed by chest compressions between geriatric and non-geriatric patients using mathematical methods and chest computed tomography: a retrospective study. *Annals of Geriatric Medicine and Research*, *22*(3), 130. https://doi.org/10.4235/agmr.2018.22.3.130

Zarb, F., Rainford, L., & McEntee, M. F. (2010). AP diameter shows the strongest correlation with CTDI and DLP in abdominal and chest CT. *Radiation Protection Dosimetry*, *140*(3), 266-273. https://doi.org/10.1093/rpd/ncq115

Zhou, Y., Zheng, Y., Wen, Y., Dai, X., Liu, W., Gong, Q., Huang, C., Lv, F., & Wu, J. (2021). Radiation dose levels in chest computed tomography scans of coronavirus disease 2019 pneumonia: A survey of 2119 patients in Chongqing, southwest China. Medicine 2021, 100, e26692. https://doi.org/10.1097/md.0000000000026692